

Electronic Supplementary Material (ESI) for Chem Commun.

This journal is © The Royal Society of Chemistry 2017

Electrical Supplementary Information

Enhanced catalytic performance of PdO catalyst prepared via a two-step method of in-situ reduction-oxidation

Wei Hu,^a Guang-Xia Li,^a Jian-Jun Chen,^b Fu-Jin Huang,^a Yang Wu,^c Shan-Dong Yuan,^c

*Lin Zhong^{*a} and Yao-Qiang Chen^{*bc}*

^a College of Chemical Engineering, Sichuan University, Chengdu, 610064, P. R. China

^b College of Chemistry, Sichuan University, Chengdu 610064, P. R. China

^c Institute of New Energy and Low-Carbon Technology, Sichuan University, Chengdu
610064, PR China.

*Corresponding authors: Yao-Qiang Chen, Email: nic7501@scu.edu.cn; Lin Zhong, Email:
zhonglin@scu.edu.cn. Tel/Fax: +86-28-85418451.

Experimental details

The La-modified γ -Al₂O₃ (denoted as LA) support is commercially available from Rhodia, containing 5 wt% of La loading. The as-received LA support was pre-calcined at 1000 °C in air for 5 h. 3 wt% palladium was introduced to LA by incipient wetness impregnation method using Pd(NO₃)₂ aqueous solution. The resulting powder was dried at 120 °C for 12 h, resulting in a sample marked as Pd/LA-C. The catalyst, denoted as Pd/LA was obtained by calcining Pd/LA-C at 550 °C in air for 3 h.

Another catalyst was prepared by in-situ reduction method. Briefly, Pd was first introduced to LA support using the same incipient wetness impregnation method as Pd/LA used. The as-prepared powder was put in air at room temperature for 12 h, and then was reduced by formaldehyde that can show excellent reducing capacity in alkaline environment at room temperature in a home-made reaction device (Scheme S1). Typically, controlled by a miniature gas circulating pump, a gas mixture consisting of about 0.5% HCHO/5% H₂O/0.5% NH₃ (25 ml min⁻¹) passed through the impregnated samples in a reaction vessel. Notably, HCHO used in our device was handled in a closed system without leaking, and the HCHO-containing mixture solution at the end of the gas circuit can be recycled after reaction. Formaldehyde, a very mild reductant, was selected to control the size and morphology of Pd NPs during the in-situ reduction. The formation of Pd nanoparticles would be governed by the balance of the nucleation rate and particle growth and the rate of Pd particle growth may be much slower than that of nucleation. As a result, the nuclei could grow to smaller particle sizes.² The

colour of the sample turned into darkness after 4 h of reaction, indicating the completely reduction of Pd²⁺ species. Then, the solid product was dried at 120 °C for 12 h resulting in a sample denoted as Pd/LA-I. Finally, the catalyst was obtained by oxidizing Pd/LA-I at 550 °C in static air for 3 h. Our two-step method was expected to firstly offer ultrafine Pd NPs with high dispersion. Due to the high uniformity and large interparticle spacing, the Pd NPs would be smoothly oxidized to PdO NPs without significant changes of particles size and dispersion even at 550 °C.^{3,4} The resulting catalyst was labelled as Pd/LA-R, and the Pd loading of Pd/LA-R was also 3 wt%.

The monolithic catalyst was obtained by coating Pd/LA or Pd/LA-R slurry that has been ball milled with an Al₂O₃ binder onto a commercial monolithic cordierite (400 channels per square inch, 6 mil). The Pd loading in the two monolith catalyst was ca. 180 ± 8 g·ft⁻³. Finally, the monolithic catalysts were dried overnight at 120 °C and then calcined at 550 °C in static air for 3 h.

The specific surface area, average pore size and total pore volume of the catalysts were measurement by N₂ adsorption-desorption experiments at the temperature of the liquid nitrogen (Autosorb SI, Quanachrome, USA). Prior to analyses, the catalysts were degassed at 300 °C in vacuum for 3 h. The specific surface area and total pore volume were calculated according to the BET and BJH method, respectively.

X-ray powder diffraction (XRD) patterns on the catalysts have been obtained by powder XRD on D/Max-rA with a Cu K α radiation ($\lambda = 0.15406$ nm) that operated at 40 kV and 25 mA. The 2 θ scanned from 20 to 90° with an interval of 0.06°.

CO chemisorption measurements were performed to measure the Pd dispersions of the catalysts. The catalysts (200 mg) were packed in a quartz U-tube reactor. Prior to CO chemisorption at room temperature, the catalysts were heated from 25 to 500 °C at a rate of 10 °C·min⁻¹ and reduced in a flow of H₂ (25 mL·min⁻¹) at 500 °C for 1 h, and then cooled to room temperature in flowing Ar (25 ml·min⁻¹), and continued purging in Ar (25 ml·min⁻¹) for 1 h prior to CO chemisorption. CO chemisorption experiments were measured by dosing 5% CO/He gas mixture at room temperature.

Transmission electron microscopy (TEM) observations were carried out on a Jeol JEM-2100 operating at 200kV to characterize the morphology of the catalysts. Typically, the catalysts powders were finely dispersed into ethanol, followed by treated with sonication for 0.5 h and by drop-casting of the dispersion onto holey carbon coated 300 mesh Cu grids.

The X-ray photoelectron spectroscopic (XPS) data were performed with an electron spectrometer (XSAM-800, KRATOS Co.) equipped with an Al K α radiation as a primary excitation. Binding energies were calculated on the basis of C 1s at 284.6 eV.

H₂-temperature-programmed reduction experiments were performed using a quartz tubular micro-reactor equipped with a thermal conductivity detector. Before measurement, the samples (100 mg) were pre-cleaned in N₂ (30 ml·min⁻¹) flow holding at 500 °C for 60 min, and then cooling to room temperature. The data was measured from room temperature to 900 °C in 5% H₂/N₂ (30 ml·min⁻¹) at a heating rate of 10 °C·min⁻¹.

Catalytic activity measurements were carried out in a fixed-bed quartz flow reactor equipped with a temperature controller instrument, and the schematic illustration of the system is shown in Fig. S1. The catalyst bed temperature was measured by using a K-thermocouple. The simulated stoichiometric NGVs exhaust gases were controlled by mass flow controllers and consisted of 1000 ppm CH₄, 3500 ppm CO, 900 ppm NO, 12.0 vol% CO₂, 10 vol% H₂O and N₂ as balance gas. The content of oxygen was added carefully to meet a stoichiometric mixed gas. The experiment was carried out at a gas hourly space velocity of 40,000 h⁻¹. The exit product composition was continuously analyzed by a FT-IR (Antaris IGS, Thermo Fisher Scientific). The conversion of product components was calculated using the following equation:

$$\text{NO conversion (\%)} = \left(\frac{[\text{NO}]_{\text{in}} - [\text{NO}]_{\text{out}}}{[\text{NO}]_{\text{in}}} \right) \times 100\%$$

$$\text{CH}_4 \text{ conversion (\%)} = \left(\frac{[\text{CH}_4]_{\text{in}} - [\text{CH}_4]_{\text{out}}}{[\text{CH}_4]_{\text{in}}} \right) \times 100\%$$

where [NO]_{in} and [NO]_{out} are the concentration of NO at the inlet and outlet, [CH₄]_{in} and [CH₄]_{out} denote volume percentage of methane at the inlet and outlet stream, respectively.

The kinetic measurements, in order to eliminate the thermal and diffusion effects, were performed to control the CH₄ and NO conversion to lower than 15%. Clearly, the reaction rate and turnover frequency (TOF) of CH₄ and NO were calculated using the following equation:

$$\text{Rate} = (FX)/(\nu W),$$

$$\text{TOF} = ([\text{Rate}]M_{\text{Pd}})/[(D_{\text{Pd}}) * (\text{Pd content in the catalyst})]$$

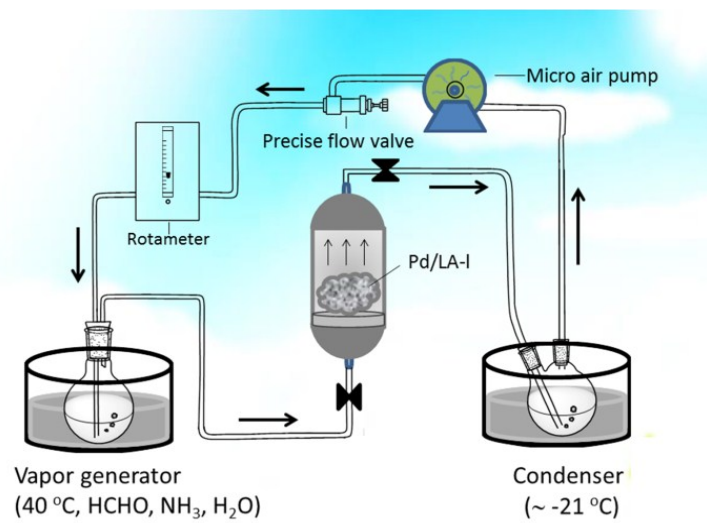
Where F is the inlet molar flow rate of the particular gas, X is the fractional conversion of gas at a particular temperature, ν is the stoichiometric coefficient of the gas, and W is the weight of the catalyst. M_{Pd} is the atomic weight of Pd (106.4 g·mol⁻¹), and D_{Pd} is the dispersion of Pd measured by CO chemisorption.¹

Table S1 Specific surface area, average pore size and total pore volume of Pd-supported catalysts.

Catalyst	S_{BET} ($\text{m}^2\cdot\text{g}^{-1}$)	Pore volume ($\text{ml}\cdot\text{g}^{-1}$)	Pore diameter (nm)
Pd/LA	138	0.51	14.9
Pd/LA-R	137	0.48	14.2

Table S2 Catalytic activities for methane and NO conversion of the catalysts.

Catalysts	Temperature programmed methane combustion (°C)					
	CH ₄			NO		
	<i>T</i> ₁₀	<i>T</i> ₅₀	<i>T</i> ₉₀	<i>T</i> ₁₀	<i>T</i> ₅₀	<i>T</i> ₉₀
Pd/LA	387	418	433	390	412	435
Pd/LA-R	324	354	372	330	349	370
Pd/LA-a	494	528	–	489	513	541
Pd/LA-R-a	440	458	550	432	454	478



Scheme S1 in situ reduction system.

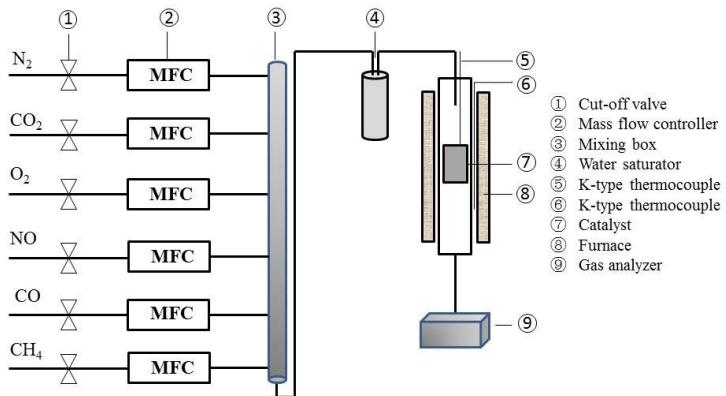


Fig. S1. Schematic illustration of the reaction activity evaluation system.

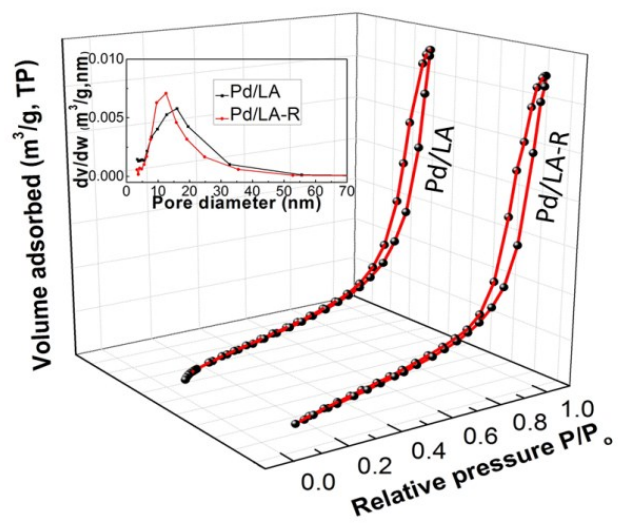


Fig. S2. Nitrogen adsorption-desorption isotherm and pore size distribution of the catalysts.

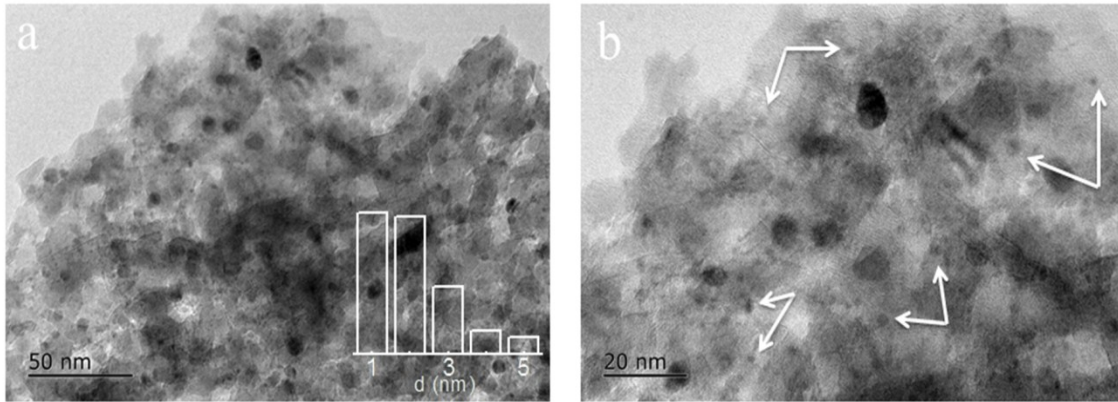


Fig. S3. TEM images of Pd/LA-I (a and b) with the corresponding size distributions of PdO NPs.

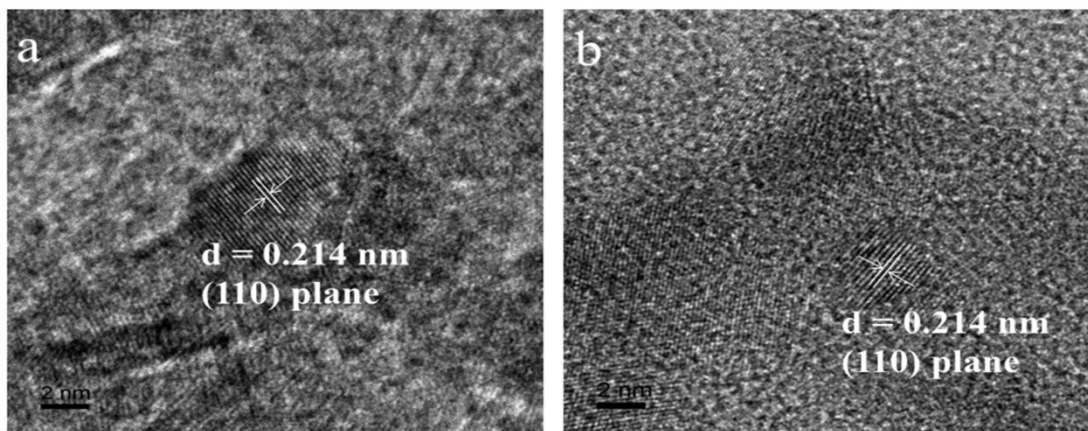


Fig. S4. HRTEM images of Pd/LA (a) and Pd/LA-R (b).

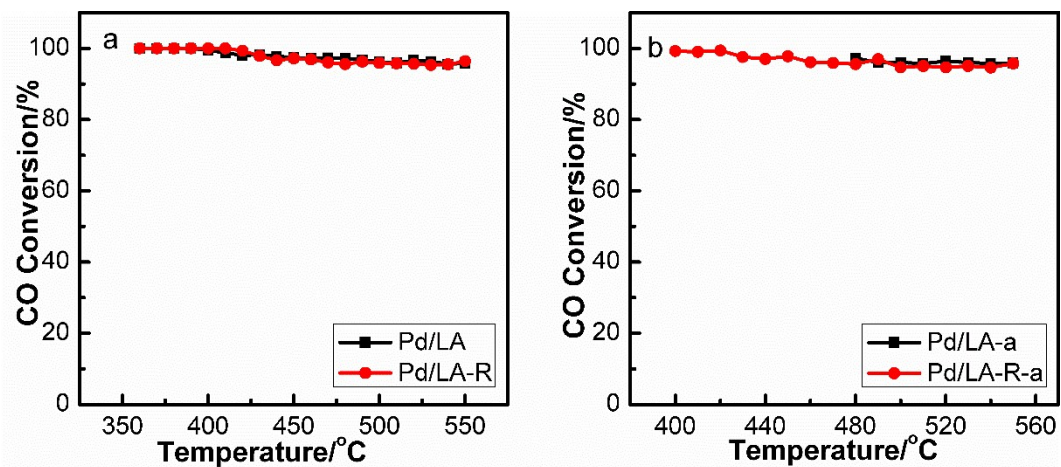


Fig. S5. Conversion of CO at different reaction temperature. Feed condition: 1000 ppm CH₄, 3500 ppm CO, 900 ppm NO, 12.0 vol% CO₂, 10 vol% H₂O and N₂ as balance gas, GSHV: 40,000 h⁻¹.

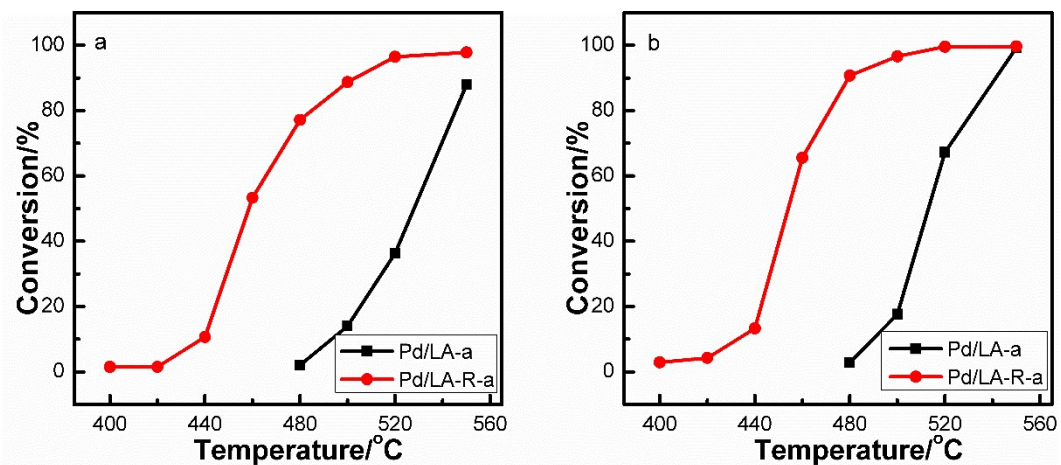


Fig. S6 (a) Conversion of CH₄ at different reaction temperature, (b) Conversion of NO at different reaction temperature. Feed condition: 1000 ppm CH₄, 3500 ppm CO, 900ppm NO, 12.0 vol% CO₂, 10 vol% H₂O and N₂ as balance gas, GSHV: 40,000 h⁻¹.

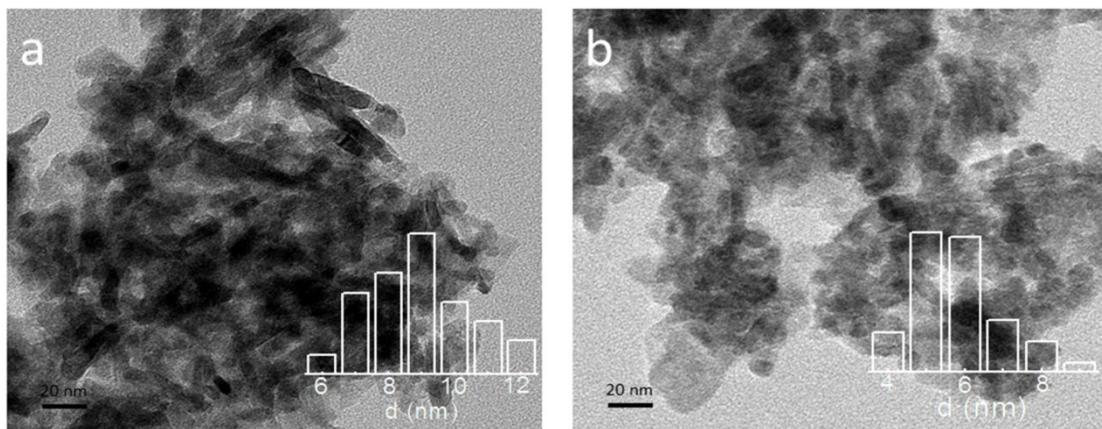


Fig. S7. TEM images of Pd/LA-a (a) and Pd/LA-R-a (b) with the corresponding size distributions of PdO NPs.

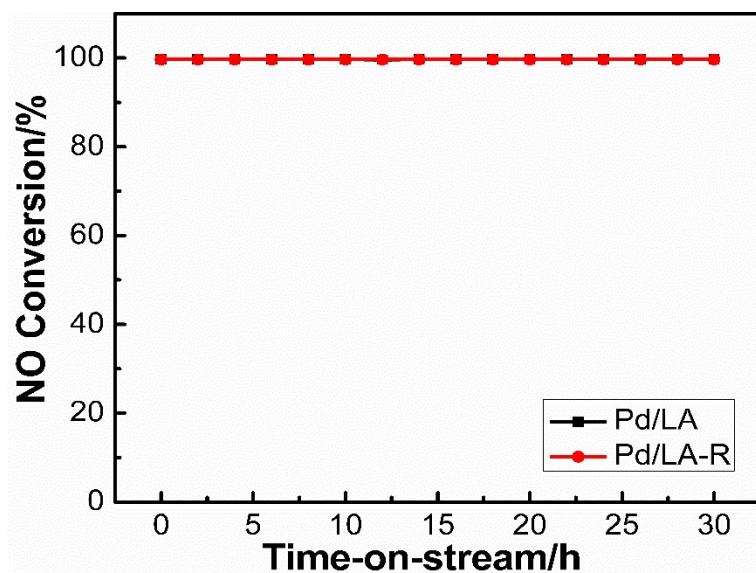
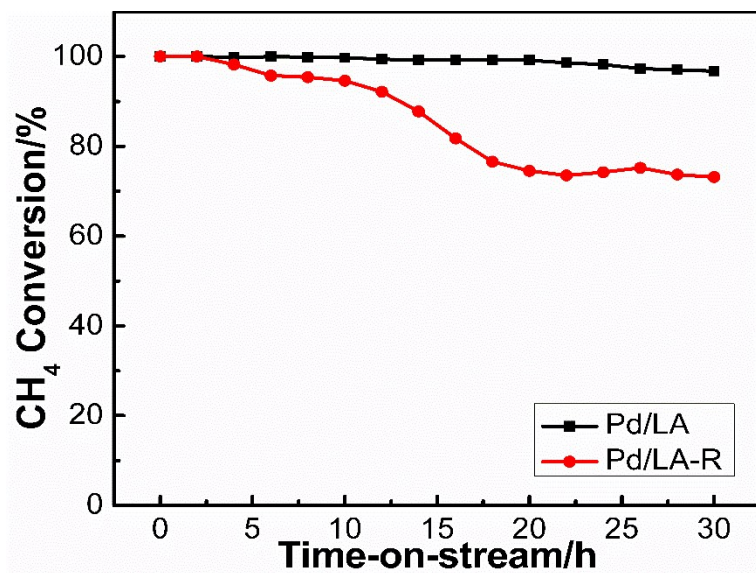


Fig. S8 Conversion versus time on stream for CH₄ and NO over Pd/LA and Pd/LA-R catalysts.

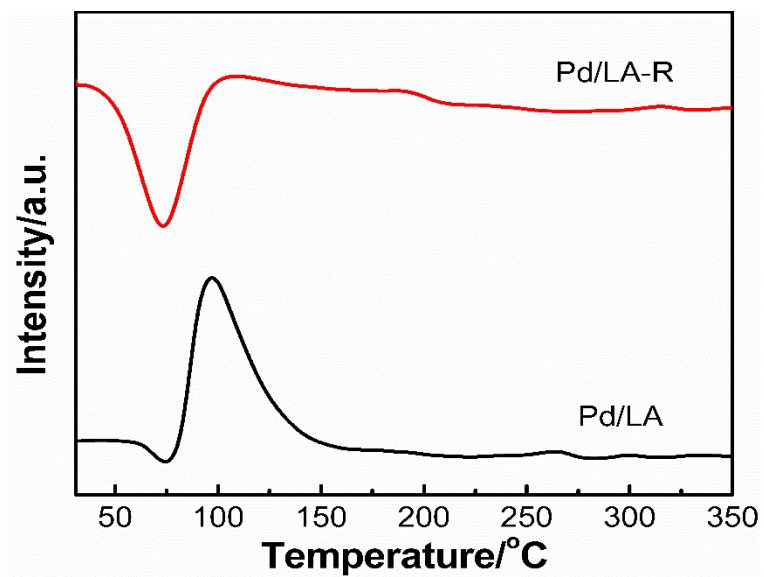


Fig. S9 H₂-TPR profiles of Pd/LA and Pd/LA-R catalysts.

Mass and heat diffusion effects

In our works, the as-prepared PdO-based catalysts were coated onto a commercial monolithic cordierite (400 channels per square inch, 6 mil). All the parameter were the same during the coating, and hence the Pd loading in the two monolith catalyst was ca. $180 \pm 8 \text{ g}\cdot\text{ft}^{-3}$ and the average washcoat thickness is about 30-50 μm . The monolith catalysts included a uniform porous washcoat with a particle size of 1-5 μm . Finally, the catalytic activity measurements of the as-prepared monolithic catalyst were carried out in a fixed-bed quartz flow reactor equipped with a temperature controller instrument.

Based on your suggestion, the absence of mass and heat transfer limitations have be assured.^{5,6} In the revised electrical supplementary information, we have added the data that is used to confirm these limitations. For CH_4 and NO , a comparison of the characteristic times helps to identify the rate controlling processes. These are as follows:

$$\text{Washcoat diffusion time: } \tau_{d,w} = R^2_{\Omega 2}/D_e;$$

$$\text{Convection time, } \tau_c = L/u;$$

$$\text{Transverse diffusion time or external mass transfer time: } \tau_e = R^2_{\Omega 1}/D_f;$$

$$\text{Reaction time: } \tau_r = C_i/ri(R_{\Omega 1}/R_{\Omega 2});$$

The existence of intraparticle (washcoat) diffusion limitations is evaluated by estimating the Weisz-Prater modulus defined by

$$\Psi = R^2_{\Omega 2}r_{obs}/D_eC_i$$

The potential contribution of external heat transfer effects to the reaction rates was explored using Mears' heat criterion, $\Delta H_{rxn}(-r_a)R_p E_a/hT^2R$,

where ΔH_{rxn} is the heat of reaction, h is the heat transfer coefficient, and R is the gas constant. The heat transfer coefficient, h , can be estimated from the Nusselt number, Nu :

$$Nu = 2 + 0.6 Re^{0.5} Pr^{1/3}$$

The thermal diffusivity, α ; the Prandtl number, Pr . The thermal conductivity, k_T ; the heat capacity, C_p .

$$\alpha = k_T/\rho C_p$$

$$Pr = \mu/\rho\alpha$$

The heat transfer coefficient, h .

$$h = (2 + 0.6Re^{0.5}Pr^{1/3})k_T/R\rho$$

The results were listed in Table S7-S10.

In Table S3, S4, S5 and S6, the characteristic time for reaction (τ_r) of four catalysts is found to be much larger than that for τ_c , $\tau_{d,w}$, and τ_e , indicating that external mass transfer is ruled out in the temperature range (conversion less than 12%). Furthermore, the existence of intraparticle diffusion limitations is evaluated by estimating the Weisz-Prater modulus, which indicates that the internal diffusion effect is negligible in our kinetics experiments. Therefore, the influence of the external mass transfer and internal diffusion resistances on the catalytic activity of Pd/LA, Pd/LA-R, Pd/LA-a and Pd/LA-R-a can be neglected.

It could also be seen that the Mears heat criterion is an order of magnitude less than 0.15 (Table S7-S10), thus external heat transfer probably does not affect the rate of reaction under the reaction conditions.

Table S3 Values of characteristic times and Weisz-Prater modulus.

CH ₄ Conversion (%)	τ_c (s)	$\tau_{d,w}$ (s)	τ_r (s)	τ_e (s)	ψ
Pd/LA-6	0.036	0.0129	0.117	0.0005	0.06
Pd/LA-8	0.036	0.0128	0.088	0.0005	0.09
Pd/LA-10	0.036	0.0128	0.070	0.0005	0.11
Pd/LA-12	0.036	0.0127	0.058	0.0005	0.13
Pd/LA-a-6	0.036	0.0115	0.105	0.0004	0.06
Pd/LA-a-8	0.036	0.0115	0.078	0.0004	0.08
Pd/LA-a-10	0.036	0.0115	0.063	0.0004	0.10
Pd/LA-a-12	0.036	0.0114	0.052	0.0004	0.12

Table S4 Values of characteristic times and Weisz-Prater modulus.

CH ₄ Conversion (%)	τ_c (s)	$\tau_{d,w}$ (s)	τ_r (s)	τ_e (s)	ψ
Pd/LA-R-6	0.036	0.0130	0.117	0.0007	0.07
Pd/LA-R-8	0.036	0.0129	0.087	0.0006	0.09
Pd/LA-R-10	0.036	0.0129	0.069	0.0006	0.11
Pd/LA-R-12	0.036	0.0128	0.057	0.0006	0.14
Pd/LA-R-a-6	0.036	0.0120	0.100	0.0005	0.07
Pd/LA-R-a-8	0.036	0.0119	0.074	0.0005	0.09
Pd/LA-R-a-10	0.036	0.0119	0.059	0.0005	0.11
Pd/LA-R-a-12	0.036	0.0118	0.049	0.0005	0.13

Table S5 Values of characteristic times and Weisz-Prater modulus.

NO Conversion (%)	τ_c (s)	$\tau_{d,w}$ (s)	τ_r (s)	τ_e (s)	ψ
Pd/LA-6	0.0360	0.0129	0.106	0.0007	0.06
Pd/LA-8	0.0360	0.0128	0.079	0.0006	0.09
Pd/LA-10	0.0360	0.0128	0.063	0.0006	0.11
Pd/LA-12	0.0360	0.0127	0.052	0.0006	0.13
Pd/LA-a-6	0.0360	0.0115	0.092	0.0005	0.07
Pd/LA-a-8	0.0360	0.0115	0.069	0.0005	0.09
Pd/LA-a-10	0.0360	0.0114	0.055	0.0005	0.12
Pd/LA-a-12	0.0360	0.0114	0.045	0.0005	0.14

Table S6 Values of characteristic times and Weisz-Prater modulus.

NO Conversion (%)	τ_c (s)	$\tau_{d,w}$ (s)	τ_r (s)	τ_e (s)	ψ
Pd/LA-R-6	0.0360	0.0130	0.117	0.0008	0.06
Pd/LA-R -8	0.0360	0.0130	0.087	0.0008	0.08
Pd/LA-R -10	0.0360	0.0130	0.070	0.0008	0.10
Pd/LA-R -12	0.0360	0.0129	0.058	0.0008	0.12
Pd/LA-R-a-6	0.0360	0.0120	0.100	0.0006	0.07
Pd/LA-R-a-8	0.0360	0.0120	0.074	0.0006	0.09
Pd/LA-R-a-10	0.0360	0.0119	0.059	0.0006	0.11
Pd/LA-R-a-12	0.0360	0.0119	0.049	0.0005	0.13

Table S7 Values of heat transfer coefficient, heat of reaction and Mears' heat criterion.

CH ₄ Conversion (%)	h (W·m ⁻² ·K ⁻¹)	ΔH (kJ·mol ⁻¹)	Mears' heat criterion
Pd/LA-6	3404.9	-628.0	0.0034
Pd/LA-8	3404.1	-630.9	0.0043
Pd/LA-10	3403.9	-633.3	0.0054
Pd/LA-12	3404.0	-641.1	0.0067
Pd/LA-a-6	4012.7	-731.7	0.0044
Pd/LA-a-8	4012.4	-734.2	0.0058
Pd/LA-a-10	4011.9	-736.2	0.0073
Pd/LA-a-12	4012.5	-738.6	0.0088

Table S8 Values of heat transfer coefficient, heat of reaction and Mears' heat criterion.

CH ₄ Conversion (%)	h (W·m ⁻² ·K ⁻¹)	ΔH (kJ·mol ⁻¹)	Mears' heat criterion
Pd/LA-R-6	2970.0	-544.9	0.0031
Pd/LA-R -8	2970.0	-549.3	0.0042
Pd/LA-R -10	2969.9	-553.2	0.0052
Pd/LA-R -12	2969.5	-558.7	0.0062
Pd/LA-R-a-6	3738.2	-682.3	0.0025
Pd/LA-R-a-8	3736.6	-687.7	0.0033
Pd/LA-R-a-10	3736.9	-694.5	0.0041
Pd/LA-R-a-12	3736.6	-700.0	0.0050

Table S9 Values of heat transfer coefficient, heat of reaction and Mears' heat criterion.

NO Conversion (%)	h ($\text{W}\cdot\text{m}^{-2}\cdot\text{K}^{-1}$)	ΔH ($\text{kJ}\cdot\text{mol}^{-1}$)	Mears' heat criterion
Pd/LA-6	1662.2	-839.5	0.010
Pd/LA-8	1661.8	-839.4	0.013
Pd/LA-10	1661.7	-839.3	0.016
Pd/LA-12	1660.8	-839.2	0.020
Pd/LA-a-6	1658.9	-835.2	0.014
Pd/LA-a-8	1658.6	-835.1	0.018
Pd/LA-a-10	1658.5	-835.0	0.023
Pd/LA-a-12	1658.6	-835.0	0.028

Table S10 Values of heat transfer coefficient, heat of reaction and Mears' heat criterion.

NO Conversion (%)	h ($\text{W}\cdot\text{m}^{-2}\cdot\text{K}^{-1}$)	ΔH ($\text{kJ}\cdot\text{mol}^{-1}$)	Mears' heat criterion
Pd/LA-R-6	1755.1	-843.0	0.0096
Pd/LA-R -8	1754.9	-842.9	0.013
Pd/LA-R -10	1754.7	-842.8	0.016
Pd/LA-R -12	1754.3	-842.7	0.019
Pd/LA-R-a-6	1759.3	-837.3	0.0076
Pd/LA-R-a-8	1758.5	-837.0	0.0099
Pd/LA-R-a-10	1758.6	-836.8	0.012
Pd/LA-R-a-12	1758.4	-836.6	0.015

Notes and references

- 1 Z. Z. Yang, N. Zhang, Y. Cao, M. C. Gong and Y. Q. Chen, *Catal. Sci. Technol.*, 2014, **4**, 3032-3043.
- 2 Y. Tan, X. Dai, Y. Li and D. Zhu, *J. Mater. Chem.*, **2003**, 13, 1069-1075.
- 3 V. P. Zhdanov, F. F. Schweinberger, U. Heiz and C. Langhammer, *Chem. Phys. Lett.*, 2015, **631-632**, 21-25.
- 4 G. Prieto, J. Zečević, H. Friedrich, K. P. de Jong and P. E. de Jongh, *Nat. Mater.*, 2013, **12**, 34-39.
- 5 P. S. Metkar, N. Salazar, R. Muncrief, V. Balakotaiah and M. P. Harold, *Appl. Catal. B*, 2011, **104**, 110-126.
- 6 D. H. Coller, B. C. Vicente and S. L. Scott, *Chem. Eng. J.*, 2016, **303**, 182-193.